Properties of the native oxide in metal/native oxide multilayers (invited)

G. S. D. Beach[a] and A. E. Berkowitz
Department of Physics and Center for Magnetic Recording Research, University of California, San Diego, La Jolla, California 92093-0401

V. G. Harris
Naval Research Laboratory, Washington, D.C. 20375-5000

F. T. Parker
Center for Magnetic Recording Research, University of California, San Diego, La Jolla, California 92093-0401

B. Ramadurai and David J. Smith
Center for Solid State Science and Department of Physics and Astronomy, Arizona State University, Tempe, Arizona 85287-1504

Multilayers composed of thin Co_xFe_{100-x} layers, each exposed successively to oxygen to form oxide surfaces, were studied to determine the structural and magnetic properties of the native oxide. Transmission electron microscopy and x-ray reflectivity provided microstructural characterization, while extended x-ray absorption fine structure and Mössbauer spectroscopy were used as local probes of the structural, chemical, and magnetic environments of the constituent atoms. The results of these analyses combined with magnetometry show an onset of magnetism in the oxide with decreasing x, near $x=90$. © *2002 American Institute of Physics.* [DOI: 10.1063/1.1452645]

There is an urgent need in the magnetic recording industry for new shielding materials which are magnetically soft with high moment and, increasingly important, high resistivity to suppress eddy current shielding at high frequencies. Recently, thin films with these properties have been fabricated using a newly introduced discontinuous metal/native oxide multilayer structure.[1] The structure consisted of thin high-moment Co_xFe_{100-x} metallic layers which have been exposed *in situ* to oxygen to form oxide surfaces. It was shown that the oxide significantly increased the resistivity of the composite, while at the same time contributing to the magnetization and soft magnetic properties.

In light of the important role played by the native oxide layer in discontinuous metal/native oxide multilayers, we have undertaken a study of the magnetic and structural properties of native oxide layers on Co_xFe_{100-x} alloys in such multilayers. Cross-sectional transmission electron microscopy (TEM) and x-ray reflection (XRR) were used to characterize the microstructure of the multilayer. Extended x-ray absorption fine structure (EXAFS) measurements provided information about the local chemical and structural environments of the Co and Fe atoms. Conversion electron Mössbauer spectroscopy (CEMS) provided further information about the local chemical environments of the Fe atoms, as well as the magnetic states of the Fe metal and oxide. Finally, combining these results with magnetometry measurements has allowed determination of the magnetization of the oxide.

Metal/native oxide multilayers were prepared as described elsewhere.[1] The notation $[Co_xFe_{100-x}(t)/\text{oxide}]_N$ denotes a structure in which each of the N unit layers consists of a nominal thickness t of Co_xFe_{100-x} which has been oxidized *in situ* in an oxygen partial pressure of 2.0 sccm for 10 s. In this article, all samples have layer thickness $t=20$ Å and $N=50$, unless otherwise noted, and a 100 Å SiO_2 capping layer is used to protect against further oxidation. Alloy compositions Co_xFe_{100-x} with $x=0$, 30, 50, and 90 were used in this study. An example of the multilayer structure is shown in the TEM micrograph of Fig. 1.

EXAFS measurements were performed using beamline X23B at the National Synchrotron Light Source at Brookhaven National Laboratory. Data were collected in fluorescence yield mode encompassing both the Fe(7112 eV) and Co(7709 eV) absorption edges, with the sample spinning at a 45° angle relative to the incident beam to minimize

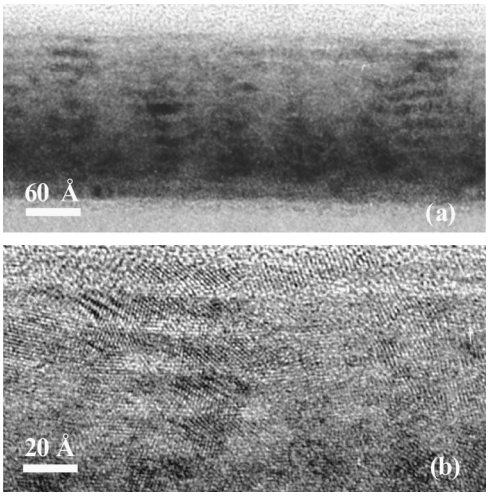

FIG. 1. (a) Low and (b) high resolution cross-sectional electron micrograph of a $[Fe(20Å)/oxide]_{10}$ multilayer sample. The regions of dark and light contrast are metal and oxide, respectively.

[a]Electronic mail: gbeach@physics.ucsd.edu

diffraction peak contamination from the single crystal Si substrate. These data were analyzed following standard EXAFS procedures,[2] leading to the Fourier transform (FT) of the data to a radial coordinate. In this form the average local environment of the absorbing atoms is reflected in the amplitude and radial distance of the Fourier peaks.[3] For samples that contain more than one inequivalent site, the data represent a superpositioning of these environments. Using the methodology of Harris *et al.*[4] one can extract the fraction of absorbing atoms in these different sites. We used this approach here to determine the atomic fraction of Fe and Co in metallic and oxide phases.

The chemical and magnetic environments of the Fe atoms were investigated using CEMS. Room temperature measurements using a ^{57}Co–Rh source were calibrated using a thick Fe film. CEMS spectra of the multilayers contained a metallic Fe (Fe^0) subspectrum and a predominantly magnetic iron oxide subspectrum, with valences determined on the basis of the isomer shift. Fitting of the spectra yielded the fraction of Fe that was metallic, and the fraction of magnetically split iron oxide.

Room temperature magnetic measurements were performed using an alternating gradient magnetometer and a superconducting quantum interference device (SQUID) magnetometer. These measurements provided saturation magnetizations of the multilayers, which will be discussed in relation to the other measurements below.

Structural analyses indicate a fine-grained metal/oxide multilayer structure. The cross-sectional TEM micrographs of Fig. 1 illustrate the structure of the metal/native oxide multilayers for $[\mathrm{Fe}(20\ \text{Å})/\mathrm{oxide}]_{10}$. Similar microstructure is observed in multilayers of other compositions. Regions of light and dark contrast correspond, respectively, to oxide and metal. Lattice fringes are visible in panel (b), and the typical grain sizes are of the order of 10–20 Å. Mössbauer data, discussed below, indicate that ~ 9 Å of metal oxidizes in each layer of this sample. The position of the XRR superlattice peaks and Kiessig fringes indicate that each metal/oxide layer has a combined thickness of 25 Å, from which we infer an oxide thickness of 14 Å. This is consistent with the TEM results. As the Co fraction is increased, the average oxide layer thickness decreases to ~ 12 Å for $x=90$, and the metallic layer thickness increases to ~ 14 Å. We note that the oxide thickness is always less than 2 unit cells of a spinel structure (spinel unit cell ~ 8 Å), suggesting that its properties are likely significantly different from bulk $\mathrm{Co}_x\mathrm{Fe}_{100-x}$ oxides.

Figure 2 contains Fourier transformed Fe and Co EXAFS data of three multilayered samples presented with similar data collected from metal and oxide standards. The standards are used for comparison purposes and in the modeling analysis. At the bottom of panels (a) and (b) are the FT data from a bcc Fe standard in which peaks are labeled to identify the neighbors in the unit cell that provide the scattering amplitude [i.e., first, second and third neighbors(N)]. This comparison is useful since the metallic phase in the samples with $x<90$ has the bcc symmetry and it allows the reader to identify the metallic peaks in the mixed phase profiles. For the FT Fe EXAFS data [Fig. 2(a)], data from a $CoFe_2O_4$ standard is used for the same reasons, while for the FT Co EXAFS data of Fig. 2(b) an fcc metal standard is plotted. The modeling of these data entails the fitting of phase and amplitude in wave vector space using linear combinations of oxide and metallic standards. The adjustable parameters are the atomic fraction of each standard and an offset voltage to account for uncertainty in the Fermi energy of the absorbing species in each site. The sensitivity of the fit depends largely on the local atomic symmetry (i.e., phase) and less on the amplitude.

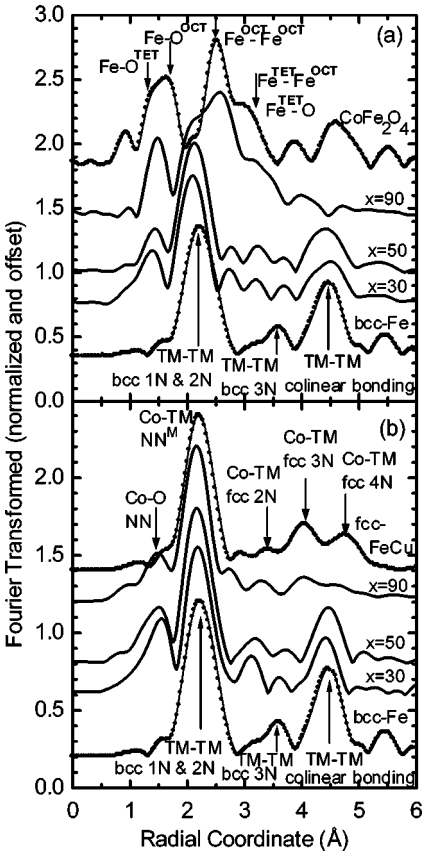

FIG. 2. (a) Fe and (b) Co Fourier-transformed EXAFS spectra for $[\mathrm{Co}_x\mathrm{Fe}_{100-x}(20\ \text{Å})/\mathrm{oxide}]_{50}$ samples of varying x (solid lines). Oxide and metal standards (dotted lines) are included for comparison.

The amplitudes of the Fourier peaks are reduced in the multilayered sample data, consistent with the reduced structural coherence lengths of the nanograined morphology. This is most significant in the Fourier peaks at higher radial coordinates. The peak appearing at $r\sim 1.4$ Å signals an oxygen neighboring the absorbing cation and is the first and most notable indicator of oxidation. In the Fe EXAFS of Fig. 2(a) this peak is seen to grow in proportion with the reduced concentration of Fe in the sample, until for $x=90$ high order cation–cation peaks appear signaling long-range order in Fe–O polyhedra. The symmetry of the oxide in this sample is consistent with the spinel structure. From the modeling of these data the metal and oxide fractions were determined (see Table I). For $x=50$ and 30, equal amounts of Fe and Co oxidize. However, for $x=90$, there is clear preferential oxidation of Fe relative to Co. Similar preferential oxidation was observed[5] in $\mathrm{Co}_{90}\mathrm{Fe}_{10}$-oxide layers recently used as

TABLE I. Fractions of Fe and Co as metal, for several $[Co_xFe_{100-x}(20\ \text{Å})/\text{oxide}]_{50}$ multilayers with varying x, from EXAFS and CEMS.

x (at. %)	Co^0 fraction (EXAFS)	Fe^0 fraction (EXAFS)	Fe^0 fraction (CEMS)
0			0.55 ± 0.01
30	0.57 ± 0.07	0.59 ± 0.07	0.68 ± 0.01
50	0.64 ± 0.10	0.65 ± 0.07	0.65 ± 0.03
90	0.74 ± 0.07	0.28 ± 0.15	0.20 ± 0.05

specular reflective layers in spin valve structures.[6] EXAFS indicates that the metal in the $x=90$ sample is mainly fcc, whereas it is bcc for the other compositions studied, consistent with the phase diagram of Co_xFe_{100-x}. Thus, in the $x=90$ sample, one might expect fcc stacking faults at which segregation of Fe-oxide may more readily occur.

Analysis of the CEMS spectra, which are sensitive only to Fe, corroborates the Fe EXAFS results, as indicated in Table I. The CEMS spectra were fitted with an Fe^0 subspectrum, along with an oxide subspectrum with a hyperfine field (HF) distribution. The Fe^0 subspectrum is consistent with Fe^0 in bulk Co_xFe_{100-x} for all samples. Additionally, for samples other than $x=90$, narrow metal subspectra indicate that there is little segregation of Co and Fe in the metal, which would lead to multiple Fe environments and thus broadening of the metallic subspectrum. Due to these facts, we assume below that the metal moment is that of bulk.

Approximately 70% of the CEMS oxide subspectrum is found in three closely spaced subspectra with strong HF splitting. The remaining oxide subspectra have a broad distribution of HFs, with a small fraction (typically $<5\%$) being nonmagnetic. In the $x=90$ sample, there is a somewhat larger fraction of weakly magnetic and nonmagnetic iron oxide. The observed HFs do not correspond to any reported values for bulk oxides, and a detailed study of the native oxide HFs will be presented elsewhere.

Room-temperature magnetization measurements of these samples exhibited saturation magnetization in excess of that expected from the fractions of metallic Co_xFe_{100-x}. This excess magnetization is attributed to the magnetic oxide phases. By using the fraction of metallic Co_xFe_{100-x} from EXAFS and CEMS, the total magnetization of the multilayer, and the total thickness of Co_xFe_{100-x}-oxide, the magnetization contributed by the oxide(s) can be calculated. The results of these calculations are shown in Fig. 3, where the entire oxide volume is used to compute an average oxide magnetization. It is clear that the oxide has a significant magnetization for all Fe-rich multilayers. The oxide magnetization increases as x is decreased from 90, saturating at a value near that of Fe_3O_4, though this is not sufficient to identify the oxide. We also note[1] that the crossover to soft magnetic properties observed in Fe-rich multilayers also occurs near

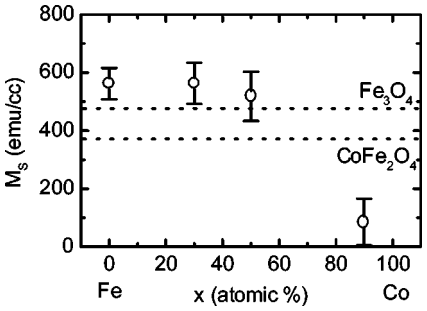

FIG. 3. Oxide magnetization in $[Co_xFe_{100-x}(20\ \text{Å})/\text{oxide}]_{50}$ samples with varying x, normalized to the oxide volume. The magnetizations of bulk $CoFe_2O_4$ and Fe_3O_4 are indicated for reference.

$x=90$. The onset of magnetism in the oxide and the onset of soft magnetic properties are well correlated, supporting the conclusions of Ref. 1 that magnetic exchange coupling of the metallic nanocrystals through the oxide leads to soft magnetic properties as per the random anisotropy model.[7] In addition, the onset of magnetism in the oxide appears to be related to the fraction of Fe in the oxide.

In summary, we have combined structural, chemical, and magnetic techniques to characterize the native oxide layers in $[Co_xFe_{100-x}(20\ \text{Å})/\text{oxide}]$ multilayer films. Under the present oxidation conditions, the oxide layer is formed from 7 to 9 Å of metal, with more metal oxidizing as the Fe content is increased. The resulting oxide layer is 12–14 Å thick and very structurally disordered. Despite this, for all compositions studied, the oxide is magnetic as indicated by both the HF and the magnetization. The oxide magnetization drops off at $x=90$, possibly due to a decreased Fe concentration in the oxide. This coincides with the loss of soft magnetic properties.[1]

This work was supported in part by the National Institute of Standards and Technology's Nanotechnology Initiative. This research was conducted in part at the National Synchrotron Light Source, which is sponsored by the U.S. Department of Energy. The authors acknowledge use of facilities at the Center for High Resolution Electron Microscopy at Arizona State University.

[1] G. S. D. Beach, A. E. Berkowitz, F. T. Parker, and D. J. Smith, Appl. Phys. Lett. **79**, 224 (2001).
[2] D. E. Sayers and B. A. Bunker, in *X-Ray Absorption: Principles, Applications Techniques of EXAFS, SEXAFS, and XANES*, edited by D. C. Koningsberger and R. Prins (Wiley, New York, 1988).
[3] The centroid of the Fourier peaks must be corrected for an electron phase shift to ascertain the true bond distance.
[4] V. G. Harris, S. A. Oliver, J. D. Ayers, B. N. Das, and N. C. Koon, Appl. Phys. Lett. **68**, 2073 (1996).
[5] M. F. Gillies and A. E. T. Kuiper, J. Appl. Phys. **88**, 5894 (2000).
[6] A. Veloso, P. P. Freitas, P. Wei, N. P. Barradas, J. C. Soares, B. Almeida, and J. B. Sousa, Appl. Phys. Lett. **77**, 1020 (2000).
[7] G. Herzer, IEEE Trans. Magn. **26**, 1397 (1990).